CHAPTER ONE HUNDRED SIXTY ONE

BOTTOM TURBULENT BOUNDARY LAYER IN WAVE-CURRENT CO-EXISTING SYSTEMS

Toshiyuki Asano* and Yuichi Iwagaki**

ABSTRACT

This study presents a new mathematical method calculating the water particle velocity in the wave-current co-existing systems. A boundary layer thickness δ_w in the co-existing system is expected to be variable with the water particle velocity ratio of wave component to current component. In this method, the boundary layer equation is solved as a free boundary problem by treating δ_w as an unknown boundary value. Several characteristics of the turbulent boundary layer such as the friction factor, friction velocity, boundary layer thickness, etc. are calculated by this method and the effect of the wave-current velocity ratio on them is discussed. Furthermore, the velocity reduction of the current due to wave superimposing is investigated.

In addition, near-bottom velocities are measured by a laser-doppler velocimeter in the pure current, the pure wave and the wave-current co-existing fields. These results are compared with calculated ones by this mathematical method.

1. Introduction

Understanding of near bottom velocity characteristics in wave and current co-existing systems is of considerable importance for sediment transport in the nearshore region, and comprehensive study of the bottom shear stress in the field is essential in developing a more acculate theory to predict nearshore current systems.

Hydrodynamics near the bottom in the co-existing field is complicated because there are mutual interactions between a current and waves. Grant-Madsen[4)] proposed a theoretical model to describe the water particle velocity and the shear stress in the wave-current co-existing field, and pointed out that the current above the wave boundary layer feels a larger resistance due to the presence of the wave than in the pure current field. This is the first theoretical study to investigate

* Research Associate, Kyoto University
** Professor, Kyoto University, M. of ASCE
Yoshida-Honmachi, Sakyo-ku Kyoto 606, Japan

not only the wave deformation by a current but also the current deformation by waves. However, their analysis left some problems to be solved.

As an important problem, we point out that convective acceleration terms were neglected in their analysis. When the velocity potential in the wave-current co-existing field is introduced, $U\partial u/\partial x$ term involved in the boundary conditions at the water surface should be considered because it is regarded to be the same order as the local acceleration term $\partial u/\partial t$. The velocity potential and the dispersion equation in the co-existing field can be deduced by considering this term.

Since the water particle velocity obtained by the boundary layer solution and that by the inviscid solution should be matched at a certain level from a bed, this term must be taken into consideration for the consistency in the analysis.

Another problem lies in how to determine the wave boundary layer thickness δ_w. This model considers the co-existing field such a way that the current feels different eddy viscosities between inside and outside of the wave boundary layer. However, the current velocity can not be estimated as long as δ_w is not determined. Grant-Madsen applied an existing knowledge on δ_w in the wave boundary layer straightforwardly to the co-existing field. Therefore, the variation of the boundary layer thickness δ_w with the wave-current composing ratio could not be considered in their analysis.

The present study proposes a new mathematical method to predict the water particle velocity in the co-existing field. By using this method, several characteristics of the turbulent boundary layer are calculated and discussed.

Finally, measurements on the near bottom velocity are carried out with a laser doppler velocimeter and the validity of this analytical method is examined by comparing with the experimental results.

2. Formulation of boundary layer equation in co-existing field

(a) Basic assumption

This study is based on Grant-Madsen's model on the wave-current turbulent boundary layer. The basic idea of their model is briefly as follows:

The current is assumed to be a fully developed flow and the associated boundary layer extends over most of the depth. Meanwhile, the wave boundary layer is confined to a relatively thin region close to the bottom. The velocity distributions both for a wave component and a current component are schematically shown in Fig.1. Consequently, the shear stress inside of the wave boundary layer is composed of wave-current interacting effect. They assumed different eddy viscosities both for inside and outside the wave boundary layer regions as follows:

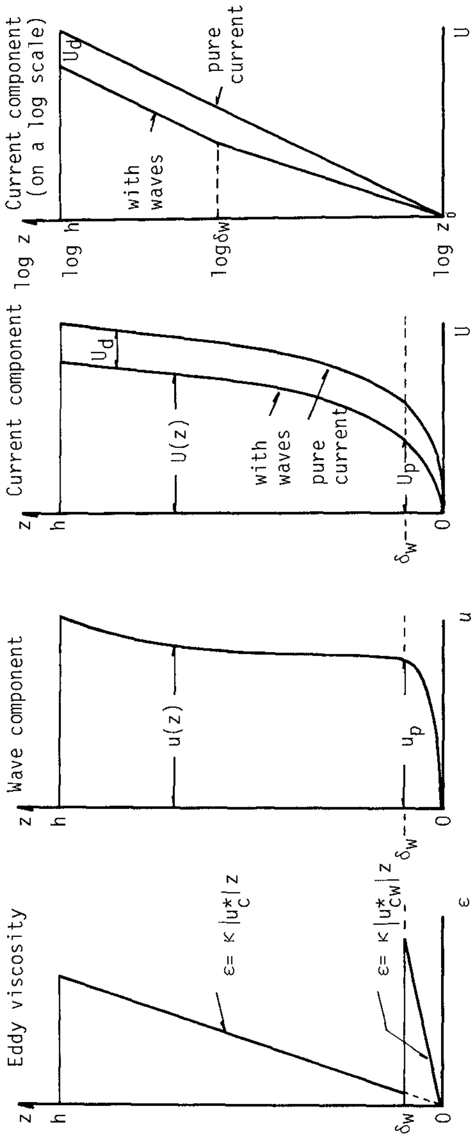

Fig.1 Profiles for eddy viscosity, wave and current components assumed in this model

$$\varepsilon=\kappa|u_c^*|z \qquad z>\delta_w \tag{1}$$

$$\varepsilon=\kappa|u_{cw}^*|z \qquad z<\delta_w \tag{2}$$

in which, κ is von Karman's constant, z the vertical coordinate, δ_w the wave boundary layer thickness , u^*_c and u^*_{cw} the shear velocities for current and wave-current motions respectively.

This assumption on the eddy viscosity, which increases linearly with the height from the bed, is not sufficient to represent the turbulent boundary layer acculately.

For the wave turbulent boundary layer, Kajiura[5] and Noda[8] proposed the elaborate theories by introducing boundary layer stratifications. For the co-existing field, Tanaka-Shuto[9] and Christoffersen[3] presented the theoretical analyses on the basis of different assumptions on the eddy viscosity distribution from Grant-Madsen's model.

Their analyses are important for refinement of the Grant-Madsen's model; however, they did not solve the above mentioned problems. Since the primary concern here is to improve the essential weakpoints of Grant-Madsen's model, this study does not consider such modifications on the eddy viscosity, and starts the analysis under the same assumptions as Grant-Madsen's theory.

The shear stress inside the wave boundary layer is calculated by the sum of the wave and current components which are presented respectively as follows:

$$\tau_w=\rho\kappa u_{cw}^* z\frac{\partial u}{\partial z} \tag{3}$$

$$\tau_c=\rho\kappa u_{cw}^* z\frac{\partial U}{\partial z} \tag{4}$$

While, outside the wave boundary layer, the shear stress is also obtained by replacing u_{cw}^* with u_c^* in Eqs.(3) and (4). The shear velocity in the co-existing field is assumed to be connected with the maximum bottom shear stress during a wave period $\tau_{cw,max}$; that is,

$$\tau_{cw,\max}=\tau_c+\tau_{w,\max}=\rho u_{cw}^{*2} =\rho\kappa u_{cw}^* z\frac{\partial(u+U)}{\partial z}\bigg|_{\max} \tag{5}$$

in which, z_0 is a constant and denotes a roughness height for fully turbulent flow.

(b) Solution for current component

Inside the wave boundary layer, the current velocity U is obtained from Eq.(4).

$$U=\frac{u_c^{*2}}{\kappa u_{cw}^*}\ln\frac{z}{z_0} \qquad z<\delta_w \tag{6}$$

The current velocity at the outer edge of the wave boundary layer U_p is given by substituting $z=\delta_w$ into Eq.(6).

$$U_p=\frac{u_c^{*2}}{\kappa u_{cw}^*}\ln\frac{\delta_w}{z_0} \tag{7}$$

Outside the wave boundary layer, the relation between the current velocity U and the current shear stress τ_c is represented with the eddy viscosity in Eq.(1) as follows:

$$\tau_c=\rho\kappa u_c^* z\frac{\partial u}{\partial z} \qquad z>\delta_w \tag{8}$$

Thus, the current velocity distribution is found from Eqs(7) and (8).

$$U=\frac{u_c^*}{\kappa}\ln\frac{z}{\delta_w}+U_p=\frac{u_c^*}{\kappa}\ln\frac{z}{\delta_w}+\frac{u_c^{*2}}{\kappa u_{cw}^*}\ln\frac{\delta_w}{z_0} \qquad z>\delta_w \tag{9}$$

(c) **Solution for wave component**

The governing equation in the wave boundary layer is as follows:

$$\frac{\partial u}{\partial t}+U\frac{\partial u}{\partial x}=-\frac{1}{\rho}\frac{\partial p}{\partial x}+\frac{1}{\rho}\frac{\partial \tau_w}{\partial z} \qquad z<\delta_w \tag{10}$$

,where the linearized convective acceleration term is involved on the left hand side.

Outside the wave boundary layer, the viscous term on the right hand side of Eq.(10) can be neglected. Thus the following equation is held at just outside the boundary layer:

$$\frac{\partial u_p}{\partial t}+U_p\frac{\partial u_p}{\partial x}=-\frac{1}{\rho}\frac{\partial p_p}{\partial x} \tag{11}$$

in which, the subscript 'p' denotes the value at $z=\delta_w$. The vertical pressure gradient is assumed to be negligible on the basis of the boundary layer approximation. The governing equation for the wave component inside the boundary layer is deduced from Eqs.(10) and (11):

$$\frac{\partial(u_p-u)}{\partial t}+U_p\frac{\partial u_p}{\partial x}-U\frac{\partial u}{\partial x}=-\frac{1}{\rho}\frac{\partial \tau_w}{\partial z}=-\frac{\partial}{\partial z}\left(\kappa u_{cw}^* z\frac{\partial u}{\partial z}\right) \tag{12}$$

In the above equation, u_p is the water particle velocity at the boundary layer edge $z=\delta_w$ and calculated from the small amplitude wave theory as follows:

$$u_p=\hat{u}_p\cos(kx-\sigma t)=\frac{H}{2}(\sigma-k\bar{U})\frac{\cosh k\delta_w}{\sinh kh}\cos(kx-\sigma t) \tag{13}$$

in which, H is the wave height, σ the angular frequency, k the wave number, h the water depth.

(d) **Free boundary problem on boundary layer equation**

The wave component in the wave boundary layer is expressed as follows:

$$u=A(z)\cos(kx-\sigma t)+B(z)\sin(kx-\sigma t) \tag{14}$$

Substituting Eq.(14) into Eq.(12), and rewriting the functions A

and B and their derivatives by $\vec{\xi}$ and $\vec{\eta}$ as

$$\vec{\xi}=\begin{pmatrix} A \\ B \end{pmatrix}, \quad \vec{\eta}=\begin{pmatrix} A' \\ B' \end{pmatrix} \tag{15}$$

we get

$$\frac{d\vec{\xi}}{dz}=\vec{\eta}, \quad \frac{d\vec{\eta}}{dz}=D\vec{\eta}+E\vec{\xi}+F \tag{16}$$

in which,

$$D=\begin{pmatrix} -\frac{1}{z}, & 0 \\ 0, & -\frac{1}{z} \end{pmatrix}, \quad E=\begin{pmatrix} 0, & -\frac{\sigma-kU}{\kappa u^*_{cw}z} \\ \frac{\sigma-kU}{\kappa u^*_{cw}z}, & 0 \end{pmatrix}, \quad F=\begin{pmatrix} 0 \\ -\frac{\sigma-kU_p}{\kappa u^*_{cw}z}\hat{u}_p \end{pmatrix} \tag{17}$$

The boundary conditions for Eq. (16) are

$$\vec{\xi}=\begin{pmatrix} 0 \\ 0 \end{pmatrix} \qquad z=z_0 \tag{18}$$

$$\vec{\xi}=\begin{pmatrix} \hat{u}_p \\ 0 \end{pmatrix}, \quad \vec{\eta}=\begin{pmatrix} 0 \\ 0 \end{pmatrix} \qquad z=\delta_w \tag{19}$$

Eq. (19) shows that the problem we discuss here is a free boundary problem because δ_w is an unknown value. The two point boundary vlaue problem as shown in Eqs. (16) ~ (19) is interpreted to be equivalent to the following characteristic equation:

$$\frac{\partial\vec{\xi}}{\partial z}+\frac{\partial\vec{\xi}}{\partial\vec{\eta}}(D\vec{\eta}+E\vec{\xi}+F)=\vec{\eta} \tag{20}$$

This partial differential equation is the so-called invariant imbedding equation, of which value lies in its wide applicability to the numerical solution of various kinds of boundary value problems. The invariant imbedding method is an initial value method for boundary value problems obtained by boundary perturbation techniques[2),7)].

An initial value problem is derived from the partial differencial equation Eq. (20) by using the following Riccati transformation on $\vec{\xi}$:

$$\vec{\xi}(z, \vec{\eta})=G(z)\vec{\eta}+H(z) \tag{21}$$

Substituting the above in Eq. (20), we obtain

$$\frac{dG}{dz}+GD+GEG=I \tag{22}$$

$$\frac{dH}{dz}+GEH+GF=0 \tag{23}$$

in which, I is a 2*2 unit matrix and 0 is 2-dimensional zero vector. The boundary condition of Eq. (18) is transformed as

$$G(z_0)=0, \quad H(z_0)=0 \tag{24}$$

in which, 0 is 2*2 zero matrix. $G(z)$ and $H(z)$ in Eqs. (22) ~ (23) are easily calculated with the initial values shown in Eq. (24). Eq. (21) is transformed as

$$\vec{\eta}(z)=G^{-1}(z)\{\vec{\xi}(z)-H(z)\}=G^{-1}(z)\left\{\begin{pmatrix}\hat{u}_p(z)\\0\end{pmatrix}-H(z)\right\} \tag{25}$$

Finally we can obtain the unknown boundary position $z=\delta_w$ as a z-value when Eq.(25) is equal to 0. After the upper boundary point $z=\delta_w$ is determined, the boundary value problem results in an initial value problem; that is, the solution of Eq.(16) can be calculated by the 'terminal condition' at $z=\delta_w$ as shown in Eq.(19).

The shear velocity of the current u^*_C is estimated by the velocity distribution of the pure current. However, if only the average current velocity in depth $\bar{U}$ is obtained for the co-existing system, u^*_C can be calculated alternatively by integrating Eq.(9) in depth and solving the resultant quadratic equation.

Thus,

$$u^*_c=\frac{-u^*_{cw}\alpha_2+\sqrt{u^{*2}_{cw}\alpha_2{}^2+4\bar{U}\kappa u^*_{cw}(h-z_0)\alpha_1}}{2\alpha_1} \tag{26}$$

in which,

$$\begin{aligned}\alpha_1&=h\ln\frac{\delta_w}{z_0}-(\delta_w-z_0)\\ \alpha_2&=h\ln\frac{h}{\delta_w}-(h-\delta_w)\end{aligned} \tag{27}$$

On the other hand, the shear velocity for the co-existing system is defined by Eq.(5), and rewrited into the following equation with invoking Eq.(6):

$$u^{*2}_{cw}=\kappa u^*_{cw}z_0\left.\frac{\partial u}{\partial z}\right|_{z=z_0}+u^{*2}_c \tag{28}$$

The above equation is a quadratic equation on u^*_{CW}, therefore if $(\partial u/\partial z)_{z=z0}$ is given, u^*_{CW} can be calculated. However, $(\partial u/\partial z)_{z=z0}$ is not known apriori, but obtained from the solution, consequently, several iterations are needed to obtain u^*_{CW}.

The boundary layer thickness δ_w is defined as the height that the maximum shear stress $\tau_{w,max}$ becomes 0. However it never coincides with exactly 0 unless z becomes infinitely large, so that, it is considered to be reasonable to define δ_w as the $\tau_{w,max}$ becomes very small relative to the value on the bottom.

In this study, δ_w is defined as the height where $(\partial u/\partial z)_{max}$ becomes 0.01 times of that on the bottom. Therefore, δ_w is varied with the multiple rate, however the solution on the water particle velocity is not affected whereever δ_w is, because only starting point differs in the calculation.

3. Calculating results and discussion

(a) Results on characteristics in wave boundary layer

In this section, several characteristics calculated by the above method are discussed and compared with those obtained by Grant-Madsen's theory.

Table 1 shows the results on several characteristics calculated from the both theories in the wave only field. The calculating conditions are as follows. The water depth h=30cm, the wave height H=10cm, the roughness height on the bottom z_0=0.1cm and the wave period T=2sec and 1.25sec for case-I and case-II, respectively. The definition of the friction coefficient f_{cw} is:

$$\tau_{cw,max} = \rho u_{cw}^{*2} = \frac{\rho}{2} f_{cw} \hat{u}_p^2 \tag{29}$$

It is clear from Table 1 that the results by the authors' method agree with those by Grant-Madsen's theory. However, results on the non-dimensional wave boundary layer thickness δ_w show some differences. In the present method, δ_w is obtained by a solution of the free boundary problem. On the other hand in Grant-Madsen's theory δ_w is assumed to be 2 or 4 times $\kappa \mid u_{cw}^* \mid /\sigma$ (in this calculation $\delta_w = 4\kappa \mid u_{cw}^* \mid /\sigma$), so that, the difference of the value is due to the estimation methods.

Table 2 shows the results in the wave current co-existing field. A little difference is seen between the results of Authors' and Grant-Madsen's, because a convective acceleration term is taken into consideration in our method.

Calculations without the convection term are also carried out by our method (indicated as Authors(2) in Table 2), and it is found that these results agree well with those by Grant-Madsen's theory.

Next, variations of the characteristics with the current velocity are discussed. Fig.2 shows the results on the friction coefficient f_{cw}, where the abscissa is a ratio of the depth averaged current velocity U to the wave celerity c calculated from the dispersion equation in the co-existing system.

The figure shows that the values of f_{cw} differ between a following current and an opposite one even if the current has a same absolute velocity. The reason is that the water particle velocity on the bottom becomes larger in the following current co-existing field than that in the pure wave field, whereas in the opposite current co-existing field the water particle velocity on the bottom becomes smaller.

Fig.3 represents the results on the shear velocity u^*_{cw}, which shows the same tendency as f_{cw}.

Fig.4 shows the results on the non-dimensional boundary layer thickness $\delta_w/(\kappa \mid u_{cw}^* \mid /\sigma)$, which indicates that the value decreases with the current velocity and the property is different from Grant-Madsen's assumption that $\delta_w/(\kappa \mid u_{cw}^* \mid /\sigma)$ is a constant independent of the current velocity.

The results on the phase precedence θ of the bottom shear stress to the water particle velocity outside the wave boundary layer are shown in Fig.5. It is found that θ decreases with the current velocity in the following current case, meanwhile θ increases a little with the current velocity in the opposite current case.

Table 1 Calculated results for characteristic values of the boundary layer in the wave-only field.
(CASE-1: $T=2$ sec, $h=30$ cm, $H=10$ cm, $z_0=0.1$ cm CASE-2: $T=1.25$ sec, $h=30$ cm, $H=10$ cm, $z_0=0.1$ cm)

		f_{cw}	u^*_{cw} (cm/sec)	δ_w (cm)	θ (rad.)
CASE-1	Authors	0.097	5.68	3.15	0.55
	Grant-Madsen	0.098	5.68	2.89	0.52
CASE-2	Authors	0.139	5.58	2.45	0.58
	Grant-Madsen	0.140	5.59	1.78	0.55

Table 2 Calculated results for characteristic values of the boundary layer in the wave-current co-existing field (CASE-1).

		f_{cw}	$\lvert u^*_{cw}\rvert$ (cm/sec)	δ_w (cm)	θ (rad.)	$\delta_w/(k\lvert u^*_{cw}\rvert/\sigma)$
$\bar{U}=30$ (cm/sec)	Authors (1)	0.144	7.13	3.55	0.51	3.91
	Authors (2)	0.154	7.38	3.55	0.54	3.78
	Grant-Madsen	0.156	7.42	3.78	0.51	4.00
$\bar{U}=-30$ (cm/sec)	Authors (1)	0.184	7.35	3.55	0.56	3.79
	Authors (2)	0.168	7.02	3.50	0.54	3.92
	Grant-Madsen	0.169	7.05	3.59	0.51	4.00
$\bar{U}=60$ (cm/sec)	Authors (1)	0.225	9.08	4.15	0.47	3.59
	Authors (2)	0.249	9.55	4.00	0.52	3.29
	Grant-Madsen	0.254	9.65	4.92	0.49	4.00
$\bar{U}=-60$ (cm/sec)	Authors (1)	0.416	9.33	4.10	0.61	3.45
	Authors (2)	0.351	8.55	3.80	0.53	3.49
	Grant-Madsen	0.354	8.62	4.39	0.50	4.00

Authors (2) denotes case of "without convection term"

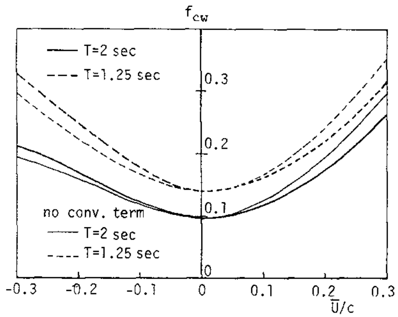

Fig.2 Friction factor f_{cw}

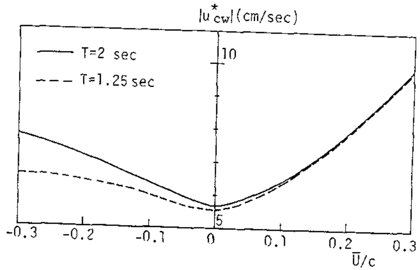

Fig.3 Friction velocity u^*_{cw}

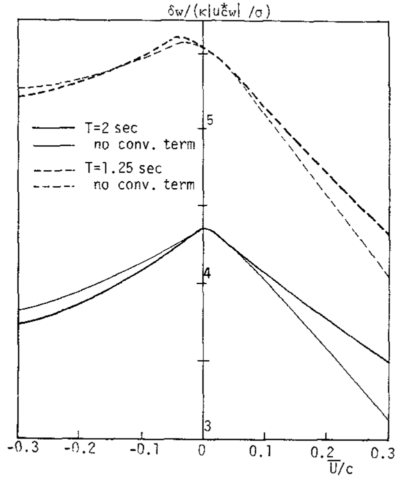

Fig.4 Non-dimensional boundary layer thickness $\delta_w/(\kappa|u^*_{cw}|/\sigma)$

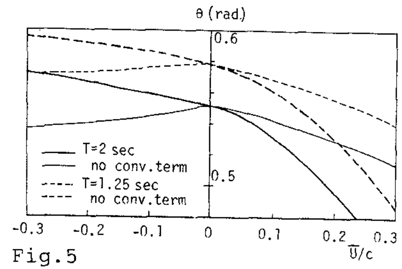

Fig.5

Phase precedence of bottom shear stress relative to water particle velocity outside boundary layer θ

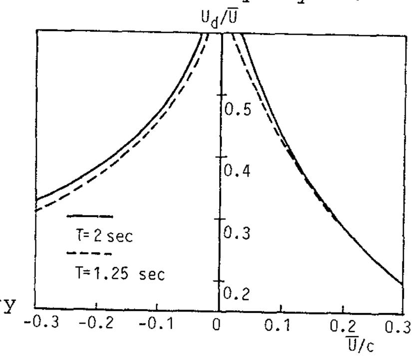

Fig.6 Non-dimensional current velocity reduction $U_d/\overline{U}$

(b) Current velocity reduction

As mentioned above, the current in the co-existing field experiences larger hydrodynamic resistance than that in the pure current field. Furthermore, the associated mean bottom shear stress is possible to differ from that in the pure current field. The current velocity without waves $U_{n.w.}$ is expressed as the well known logarithmic law.

$$U_{n.w.}=\frac{u_c^*}{\kappa}\ln\frac{z}{z_0} \tag{30}$$

Meanwhile, the current velocity in the co-existing field is represented in Eq.(9). Thus, the reduction of velocity U_d due to wave superimposing above the wave boundary layer is obtained by subtracting Eq.(9) from Eq.(30) as follows:

$$U_d=U_{n.w.}-U=\left(\frac{u_c^*}{\kappa}-\frac{u_c^{*2}}{\kappa u_{cw}^*}\right)\ln\frac{\delta_w}{z_0} \tag{31}$$

The above equation shows that the reduction depends directly on the wave boundary layer thickness δ_w.

This method treats δ_w as a variable with the wave-current composing ratio and estimates it as a solution of the free boundary problem. Consequently, this method is rational to estimate the current velocity reduction. The calculated results on the non-dimensional reduction velocity U_d/U are shown in Fig.6.

(c) Instantaneous water particle velocity

Fig.7 and Fig.8 are the calculated results on the distribution of water particle velocity for a following and an opposite current cases respectively. The thin curves in the figure show the results calculated from the authors' method without the convective acceleration term. In addition, the results calculated from Grant-Madsen's theory are shown by the dotted curves for comparison. It is found from the figure that the convection term decreases the absolute values of water particle velocity in the following current case, and increases those in the opposite current case.

The effect of the convection term increases as U/c becomes large, because the ratio of the convective acceleration term $U\partial u/\partial x$ to the local acceleration term $\partial u/\partial t$ becomes U/c. In the actual nearshore regions, however, the value of U/c is usually small, therefore it occurs rather seldom that the convection term plays an important role.

4. Measurements on near bottom velocity

(a) Experimental apparatus and procedure

The experiment was carried out in a 27m long, 0.5m wide and 0.7m high wave tank, in which circulating flow could be generated by a power pump. The water depth was kept constant at 30cm. Test runs were conducted under the conditions that the wave period was 1.67sec, the wave height were 6.3 8.5cm. All the cases of current used in the tests were in the opposite direction to the wave propagation. Two dimensional

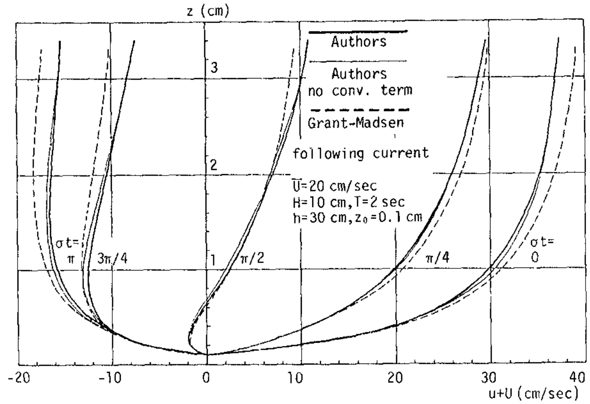

Fig.7 Distributions of horizontal water particle velocity in co-existing field (following current)

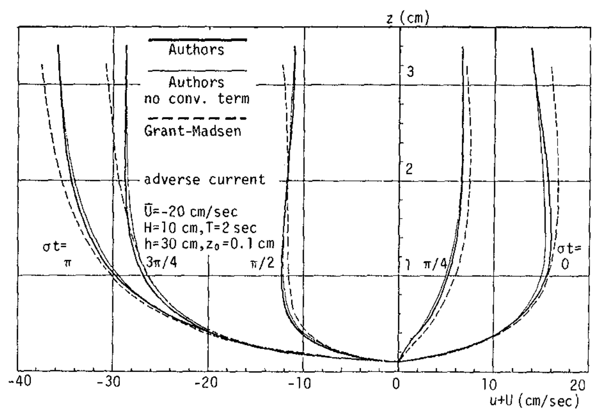

Fig.8 Distributions of horizontal water particle velocity in co-existing field (adverse current)

roughness elements of 2mm × 2mm in cross section and 15mm interval were added on the bottom.

Water particle velocities were measured with a lazer-doppler velocimeter, and at the same location water surface variations were detected simultaneously by a capacitance type wave gauge. The measuring points were located at the lowest 1.4mm ~ 1.7mm above the top of the artificial roughness and at the highest 100mm above that. The total measuring points were 21 ~ 23 for each test case. The test conditions are summarized in Table 3, and a schematical view of the experimental apparatus is shown in Fig.9.

(b) **Current component velocity**

The current component velocity in the co-existing system is defined as the time averaged velocity during a wave period. Fig.10 shows the current component velocities both in the pure current field and in the co-existing field.

The velocity reduction of the current component in the co-existing field is clearly seen from the figure.

The dotted line shows the calculated results from the authors' theory, where only the depth averaged velocity of the pure current and the wave conditions are given as inputs of the calculation.

(c) **Instantaneous water particle velocity**

Fig.11 shows the experimental results in the pure wave field, and the calculated results by the authors' and Grant-Madsen's theories are also shown for comparison.

The experimental results take larger values than the calculated ones at the phases 0 and $\pi/4$ in the region of $z < 2$cm, and the distributions show over-shooting phenomena that the velocity in the boundary layer exceeds the outer velocity. Furthermore, the experimental results become smaller than the calculated ones especially at the phase $3/4\pi$ and π in the region of $z < 5$mm.

Similar results were found in experimental results performed by Bakker and van Doorn[1], who measured water particle velocities under the similar experimental conditions to those of this study.

It also seems to be a reason of the disagreement that the water particle velocities under this test condition were not enough large to generate fully rough turbulent flow near the bottom.

Fig.12 shows the results in the wave-current co-existing field. The agreement between the calculated and experimental results seems to be better in the co-existing field than that in the pure wave field.

The reason can be explained by the fact that in the co-existing field the turbulent flow was produced close to the bottom due to superimposing current, while in the pure wave field under these experimental conditions the laminar sublayer occupied some width on the bottom.

In order to improve the mathematical model for predicting the experimental result more accurately, it is necessary to solve the

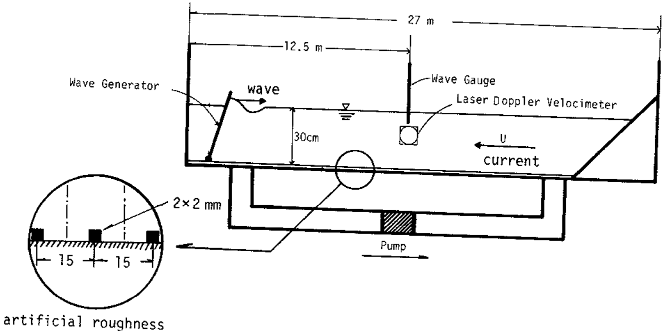

Fig.9 Experimental apparatus

Table 3 Experimental conditions.

		$\bar{U}$ (cm/sec)	H (cm)	T (sec)	h (cm)
CASE-I	wave-only	0	8.52	1.67	30
	current-only	−20.0	—		
	co-existing	−17.4	7.74		
CASE-II	wave-only	0	7.99	1.67	30
	current-only	−30.3	—		
	co-existing	−25.9	7.49		
CASE-III	wave-only	0	8.22	1.67	30
	current-only	−41.6	—		
	co-existing	−36.7	6.30		

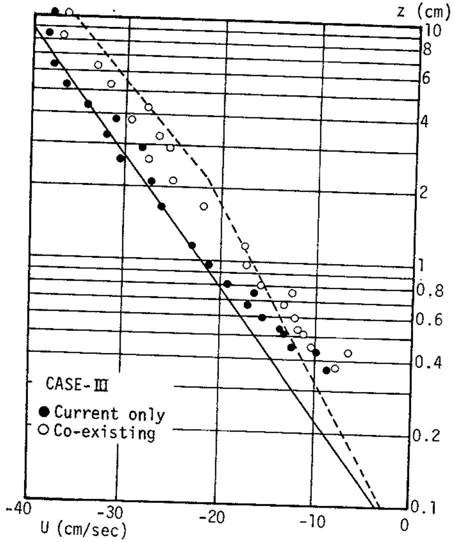

Fig.10 Distributions of current component in pure current and co-existing fields

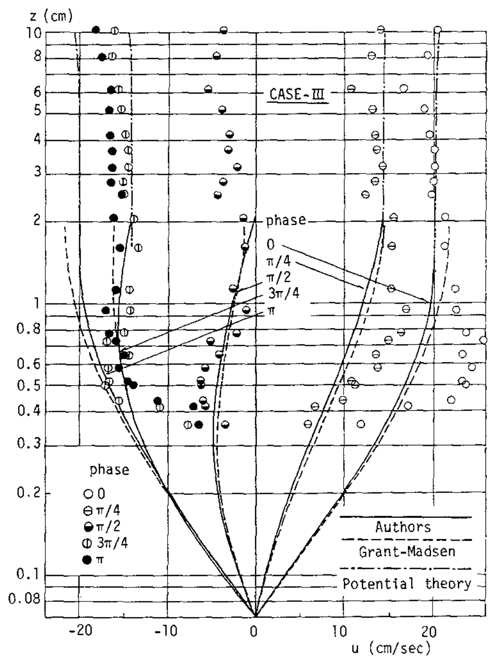

Fig.11 Comparisons between experimental results and theoretical ones in pure wave field

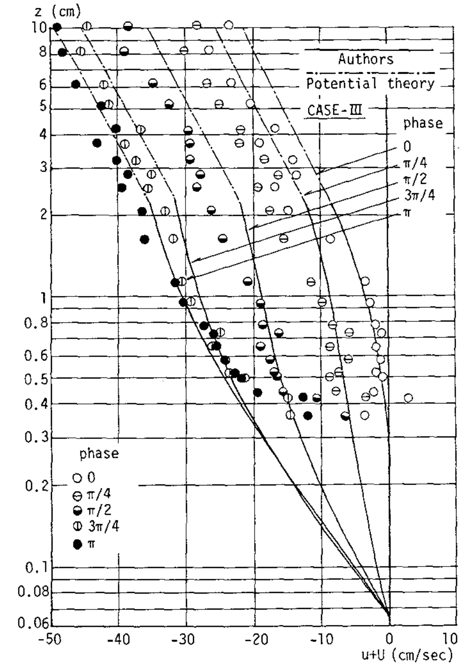

Fig.12 Comparisons between experimental results and theoretical ones in co-existing field

several important problems remained even in the pure wave boundary layer.

One important problem is the finite amplitude effect of waves on the water particle velocity in the wave boundary layer. Another problem lies in the assumption on the eddy viscosity. How to determine the roughness height z_0 in oscillating flow is also one of the problems to be solved.

5. Conclusions

This study proposes a new mathematical method to predict near bottom water particle velocities in the wave-current co-existing field. Since this method is capable of expressing the variation of the boundary layer thickness with the wave-current velocity ratio, several characteristics of the boundary layer and the current velocity reduction due to superimposing waves can be estimated reasonably by this method.

Moreover, measurements on the water particle velocity above the artificial rough bottom were carried out in the pure wave, the pure current and the wave-current co-existing fields.

After comparing the calculated results with the experimental data, it was found that this method predicts well the experimental results, however some disagreements between them are obtained. These are partly due to the assumption on the eddy viscosity which is proportional to the height from the bottom, and in addition, due to neglecting the finite amplitude effect of waves.

Acknowledgement

This study is part of the research sponsored by the Grant-in-Aid for Scientific Research of the Ministry of Science, Culture and Education. The authors wish to express their appreciation to Mr. H. Okamoto, former graduate student at Department of Civil Engineering, Kyoto University, for his assistance in performing the experiments.

References

1) Bakker, W.T. and Th. van Doorn : Experimental investigation of near bottom velocities in water waves without and with a current, Delft Hydraulic Laboratory, M1423, part 1, p. 66, 1981.
2) Bellman, R. : Methods on nonlinear analysis, Mathematics in Science and Engineering, Vol. 61-II, Academic Press, p.261, 1973.
3) Christoffersen, J. B. : Current depth refraction of dissipative water waves, Inst. of Hydrodynamics and Hydraulic Engineering (ISVA), Technical University of Denmark, Paper No.30, p.177, 1982.
4) Grant, W.D. and O.S. Madsen : Combined wave and current interaction with a rough bottom, J. of Geophysical Research, Vol. 84, No. C4, pp.1797-1808, 1979.
5) Kajiura, K. : A model of the bottom boundary layer in water waves,

Bull. of Earthquake Res. Inst., Vol.46, pp.75-123, 1968.
6) Kemp, P.H. and R.R. Simons : The interaction between waves and a turbulent current : waves propagating with the current, J. Fluid Mech., Vol.116, pp.227-250, 1982.
7) Mayer, G.H. : Initial value methods for boundary value problems, theory and application of invariant imbedding, Mathematics in Science and Engineering, Vol.100, Academic Press, p.220, 1973.
8) Noda, H. : On the oscillatory flow in turbulent boundary layers induced by water waves, Bull. Disas. Prev. Res. Inst., Kyoto Univ., Vol.20, Part 3, No. 176, March, pp.127-144, 1971.
9) Tanaka, H. and N. Shuto : Friction coefficient for a wave current co-existing system, Coastal Engg. in Japan, Vol.24, pp. 105-128, 1981.